Environ Monit Assess (2023) 195:688
https://doi.org/10.1007/s10661-023-11248-z

RESEARCH

3D modelling of surface spreading and underground dam groundwater recharge: Egri Creek Subbasin, Turkey

Yavuz Sahin · Gokmen Tayfur

Received: 5 December 2022 / Accepted: 13 April 2023 / Published online: 18 May 2023

Abstract This study investigated surface spreading and underground dam recharge methods to replenish groundwater in Turkey's Egri Creek Sub-basin of the Kucuk Menderes River Basin. A three-dimensional numerical model was employed for this purpose. Field and lab data are provided to the model for realistic simulations. Pumping test results were used to determine the aquifer parameters. The laboratory works involved sieve analysis, permeability tests, and porosity and water content prediction. The numerical model's boundary conditions were determined from the geological and hydrogeological characteristics of the study area. Initial conditions were expressed regarding water content and pressure head in the vadose zone. The numerical model was satisfactorily validated by simulating water levels in three different pumping wells in the study area. Seven different scenarios, each having a different pool size, were investigated for the surface spreading recharge method. The results showed that a pool size of 30×30 m with a 6-m depth basin was the most optimal choice, raising the groundwater level to about 29.3 m. On the other hand, it was found that an underground dam could raise the levels by an average of 9.5 m, which might not be significant to warrant the construction.

Y. Sahin
Izmir Institute of Technology, The State Water Works (DSI), Izmir, Turkey
e-mail: yavuzsahin1905@gmail.com

G. Tayfur (✉)
Department of Civil Engineering, Izmir Institute of Technology, Izmir, Turkey
e-mail: gokmentayfur@iyte.edu.tr

Keywords Recharge · Surface spreading · Underground dam · Numerical model · Artificial recharge scenarios

Introduction

Groundwater is one of the important resources in agriculture, industry, and domestic consumption. About 43% of groundwater is used in global agricultural activities (Siebert et al., 2010). Due to climate change and unconscious human activities, groundwater resources are rapidly diminishing. In many parts of the world, especially arid and semi-arid regions, groundwater extractions exceeded groundwater recharge, resulting in major level decreases (Al-Muttair & Al-Turbak, 1991; Masoud et al., 2019).

It is not easy to replenish groundwater storage since it depends on several factors, such as climate, hydrology, meteorology, and hydrogeology (Bouwer, 2002; Jarraya-Horriche et al., 2020). When natural recharge processes become inadequate, artificial methods can be used to accelerate the natural replenishment of groundwater (Boochs & Billib, 1994). Artificial recharge can be accomplished by rainwater harvesting (e.g., ditches, recharge wells, harvesting in cistern from hillsides, subsurface dams, farm ponds, historical large well across streamlets, and check dams) or by pumping excess water from rivers and/or lakes to suitable aquifer system either by surface infiltration in basins (e.g., surface spreading basins and recharge pits and shafts) or by pumping directly into the ground (e.g., recharge wells) or by constructing subsurface dams (e.g., underground dams) (https://www.geographynotes.com/geology-2/rainwater-harvesting/top-9-methods-of-groundwater-recharge-geology/1573). This study focuses on the surface spreading basins and underground dam recharge methods.

The common method of artificial recharge of groundwater is the surface spreading basins (SSB), where recharge water is allowed to infiltrate down to water table from natural or man-made depressions (Phillips, 2003; Izbicki et al., 2007). Maximising infiltration rate is the main concern in the water spreading, and hence the underlying aquifer should be unconfined (Light, 1994). Infiltration rates are closely related to the physical and chemical characteristics of soil and subsurface conditions. Physiography and properties of surface and subsurface soils can be used as a guide for assessing such conditions (Gelebo et al., 2022; Richter & Chun, 1959; Schiff & Dyer, 1964). The SSB method requires extensive land areas, surface soil with high vertical permeability, periodic maintenance to prevent clogging, and little or no water pre-treatment (Kimrey, 1989). On the other hand, high evaporation losses and groundwater vulnerability to surface contamination are the main concerns. Another spreading method is subsurface spreading, which can minimize evaporation losses and required land area. However, in such an application, initial costs are high, and it is difficult to clean these structures (Reddy, 2008).

Underground dam (UD) is also an artificial recharge method that can prevent running off groundwater beneath the ground; the water is stored upstream of the dam (Foster & Tuinhof, 2004; Nilsson, 1988). The UD prevents losses of high evaporation rates, reservoir contamination, siltation risks, etc. (Boochs & Billib, 1994). The UDs are usually constructed in arid regions where irregular rainfall is observed. Well-defined and narrow valleys are preferred for locating UDs. From a hydrogeological point of view, river beds consisting of sand and gravel are considered the best localities, where suitable storage and flow characteristics can be observed. In Turkey, studying underground dam construction is a new topic. The first underground dam is constructed in Cesme, Izmir, in 1998, followed by the ones in Kırıkkale in 2003 and in Ankara in 2005 (Apaydın, 2009, 2014).

The purpose of this study is to assess potential for artificial recharge of groundwater in a subbasin of the Kucuk Menderes River Basin (KMRB) in western Turkey. The KMRB has faced continuous groundwater level decreases for the past 30 years. Most of the groundwater (86.8%) in the basin is used for irrigation in the summer season when the Kucuk Menderes River and its tributary streams are mostly dry (Yagbasan, 2016). Streams in the basin generally run from October through April in response to precipitation received in this period. Thus, extensive pumping in summer seasons has reduced the groundwater levels significantly, thereby allowing a groundwater storage potential to be recharged in the wet seasons when the streams are running. A reasonable way to achieve this is to apply the methods of artificial recharge of groundwater. These methods aim to store water for later use when water is inadequate. This study explores the potentiality of the SSB and the UD recharge methods to replenish groundwater in the Egri Creek Subbasin of the KMRB by employing field and laboratory data together with the three-dimensional numerical model.

Study area and data

Study area

Egri Creek Sub-basin is one of the sub-basins of Kucuk Menderes River Basin (KMRB), which is surrounded by the Kucuk Menderes River in the north and steep mountain ridges in the other directions, and the elevation ranges from 100 to 1550 m (see Fig. 1a). Egri Creek, which originates at the mountains in the south of Gokcen, has a total drainage area of 130.3 km^2.

Agricultural irrigation and domestic activities have caused a dramatic decline in groundwater levels over the years. Before 1960s, the groundwater level ranged from 13 to 25 m and then decreased to 35–60 m in the period 1960–2018. In the study area, the groundwater level is currently approximately 35 m. Figure 2 shows the monthly groundwater level change in the study area (the well locations are given in Fig. 1b) for the period of 1966–2018 (DSI, 2016; DSI Records, 2019; Yazicigil et al., 2000).

Geology

The study area is located near Gokcen Region, which lies between Tire in the west and Adagume in the

(a)

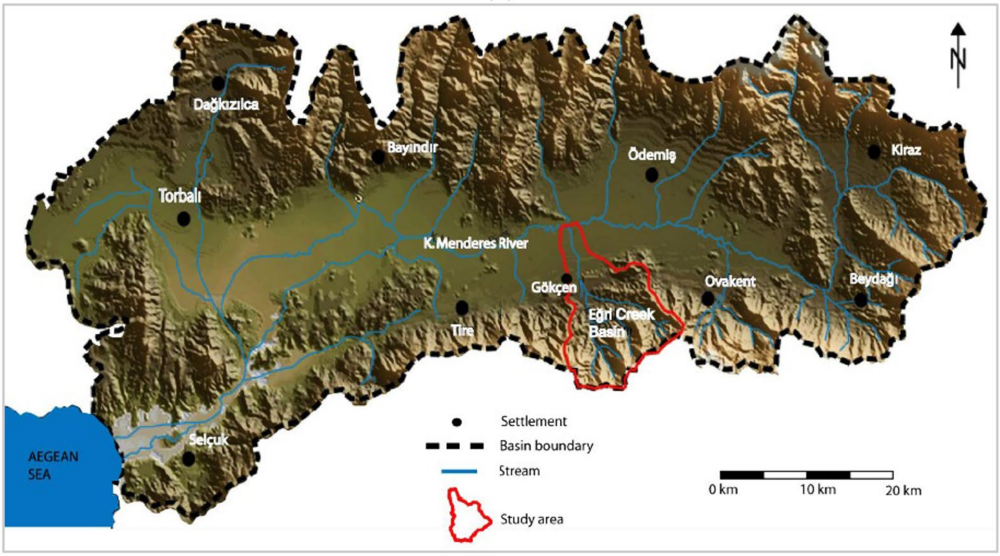

(b)

Fig. 1 **a** Location of Egri Creek Sub-basin in Kucuk Menderes River Basin; **b** location of the study area in Egri Creek Sub-basin

east. As seen from the geological map, represented in Fig. 3, there are two main lithologic units: alluvial fan deposits and Menderes Massif metamorphic.

The most characteristic feature in the area is the presence of alluvial fans. The thickness and slope of the alluvial fans seem to increase from Tire towards the eastern parts. The thickness appears to be about 180 m. In addition, the alluvial fan material has been transported over long distances into the plain. The main mechanism controlling the formation of the alluvial fans is the faulting. Along the margins of the area, Menderes Massif metamorphics are widely observed. Especially in Gokcen region, alternation of schists and gneiss are dominant, whereas marble

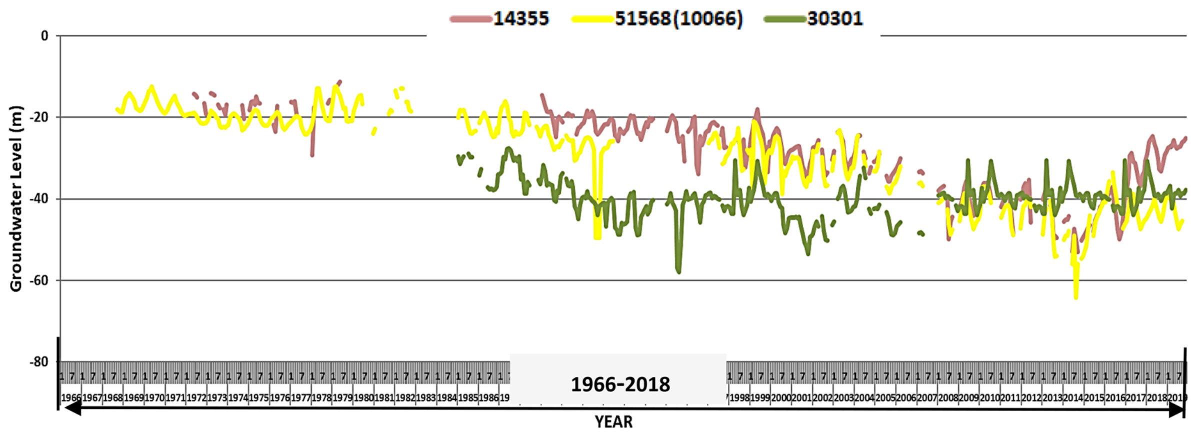

Fig. 2 Monthly groundwater level change in the study area from 1966 to 2018 (Yazicigil et al., 2000)

is not found. The faults examined in Gokcen region stretch in the E-W direction. The largest fault can be followed along Camlica, Sarilar, Isikli, Boynuyogun, and Karacaali villages, not continuously but discretely. To the west, this joins with another fault that reaches Belevi. Fault steepness, the presence of thick alluvial deposits and Neogene units are the main indicators for the occurrence of the fault. Based on the lineation studies, the fault appears as a left-lateral normal fault. The details can be obtained from Yazicigil et al. (2000) and the Kucuk Menderes River Basin master plan report (DSI, 2016).

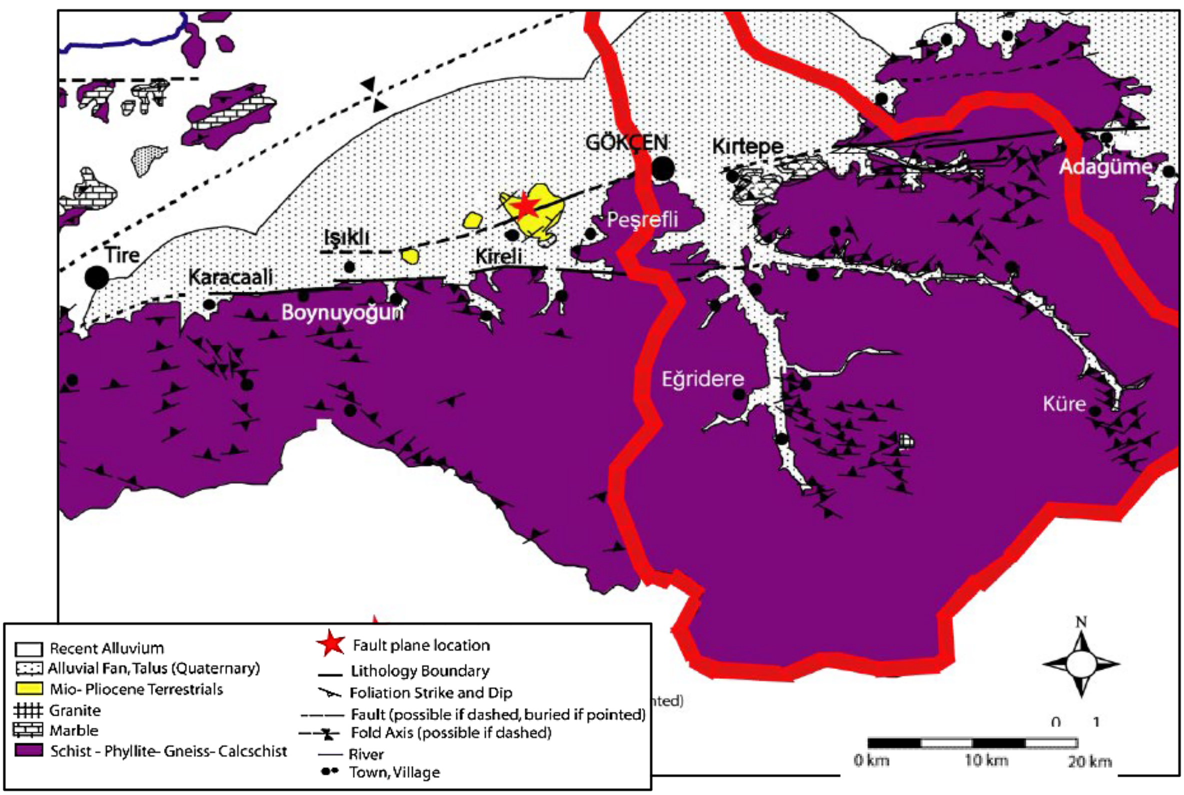

Fig. 3 Geological map of Gokcen region, the study area

The study area consists of two main geological units. The basement rocks of schist and gneiss and the overlying alluvial fan deposits. In terms of water-bearing capacities, the alluvial fan deposits are the main units that allow the flow of groundwater due to high porosity. The other unit, which is composed of schist and gneiss, forms an impervious boundary where no flow is observed. Hence, the flow takes place within the alluvial fan deposits that consist of a combination of talus, gravel, sand, and silt with alternation of clay deposits and a thickness of about 180 m (Sayit & Yazicigil, 2012). The groundwater flow occurs from south to north direction where it eventually reaches the Kucuk Menderes River (Sayit & Yazicigil, 2012). Exploration well logs indicate that the subsurface geology does not contain any impending layers with a significant thickness or extent, and therefore the aquifer in the study area is defined as unconfined, whose thickness ranges from 26 to 148 m. The thickness of the unsaturated zone decreases from south (~60 m) to north (~15 m), with an average thickness of 45 m (Sayit & Yazicigil, 2012). Conditions of a thick unsaturated zone, the presence of alluvium and permeable material, as well as the existence of an unconfined aquifer, suggest the suitability of the artificial recharge in the study area.

Meteorological data

The study area is under the influence of the Mediterranean (Aegean) climate, where summers are hot and dry while winters are mild and rainy (Yazicigil et al., 2000). Since Odemis meteorological station is the closest station to the sub-basin (about 12 km) and topographically at the same elevation, the meteorological data used in this study are obtained from this station. The maximum and minimum temperatures are measured as 30 and 3 °C, respectively, and the annual average temperature is about 16 °C. Average, minimum, and maximum monthly temperature values obtained for the period of 1960–2018 are shown in Fig. 4.

As a characteristic of the Mediterranean climate, precipitation is high in winter but low in summer. The seasonal distribution of average annual precipitation is given in Fig. 5. The average monthly precipitation is about 52 mm. The annual total precipitation is about 620.5 mm. Based on the long-term data from the Odemis station, the maximum and minimum monthly precipitations are measured as 333.7 and 2 mm, respectively. Figure 6 illustrates the monthly average, maximum, and minimum precipitation values for 1960–2018.

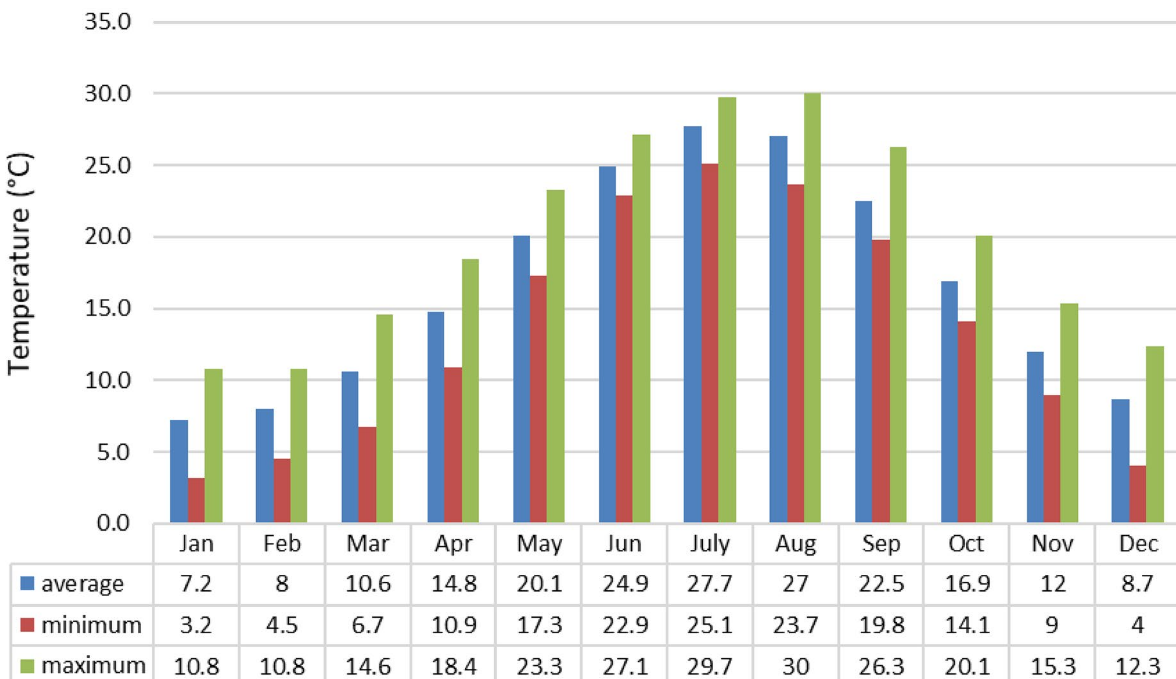

	Jan	Feb	Mar	Apr	May	Jun	July	Aug	Sep	Oct	Nov	Dec
average	7.2	8	10.6	14.8	20.1	24.9	27.7	27	22.5	16.9	12	8.7
minimum	3.2	4.5	6.7	10.9	17.3	22.9	25.1	23.7	19.8	14.1	9	4
maximum	10.8	10.8	14.6	18.4	23.3	27.1	29.7	30	26.3	20.1	15.3	12.3

Fig. 4 Average, minimum, and maximum monthly temperature values for Odemis Station

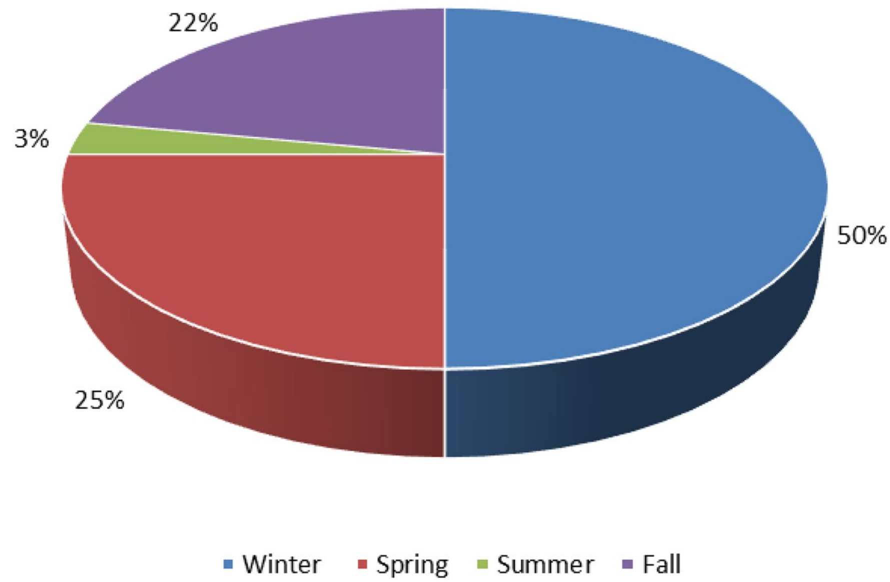

Fig. 5 Seasonal distribution of average annual precipitation for Odemis Station

The monthly maximum evaporation value is measured as 415.4 mm in July, which is the hottest month. The long-term data indicate that the annual total evaporation is measured as 1509.3 mm. The monthly average, minimum, and maximum evaporation data obtained for 1960–2018 are shown in Fig. 7.

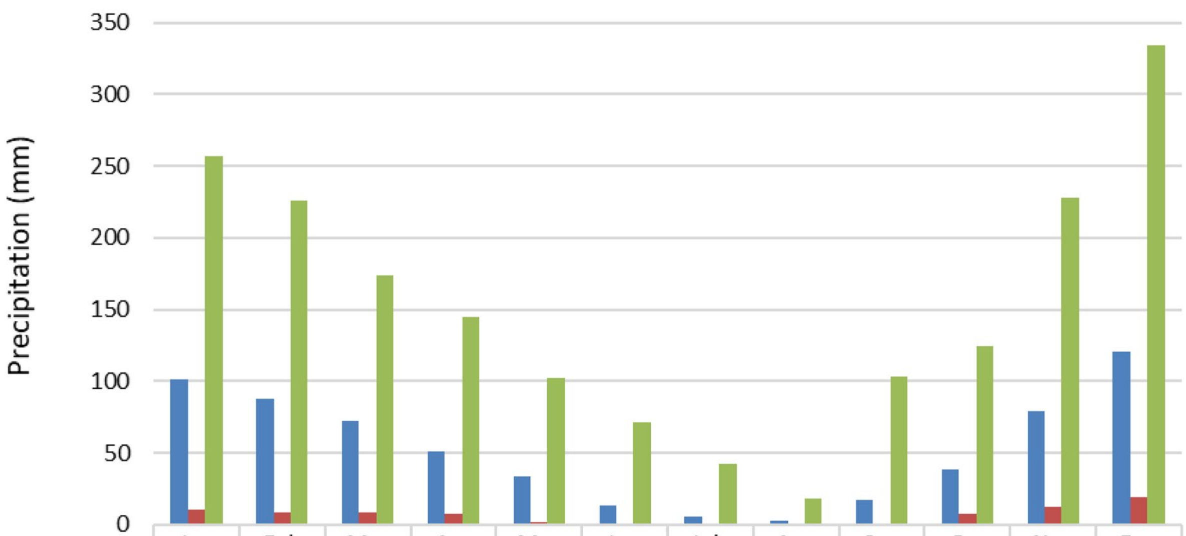

	Jan	Feb	Mar	Apr	May	Jun	July	Aug	Sep	Oct	Nov	Dec
average	101.5	87.9	72.1	51.1	33.6	13.6	5.4	2.4	17.5	38.3	79	120.1
minimum	10	8.3	8.5	7.6	2	0	0	0	0	7.4	12.5	19.1
maximum	257.1	225.5	173.7	144.3	102.5	71	42.6	17.9	103.1	124.7	227.4	333.7

Fig. 6 Average, minimum and maximum monthly precipitation values for Odemis Station

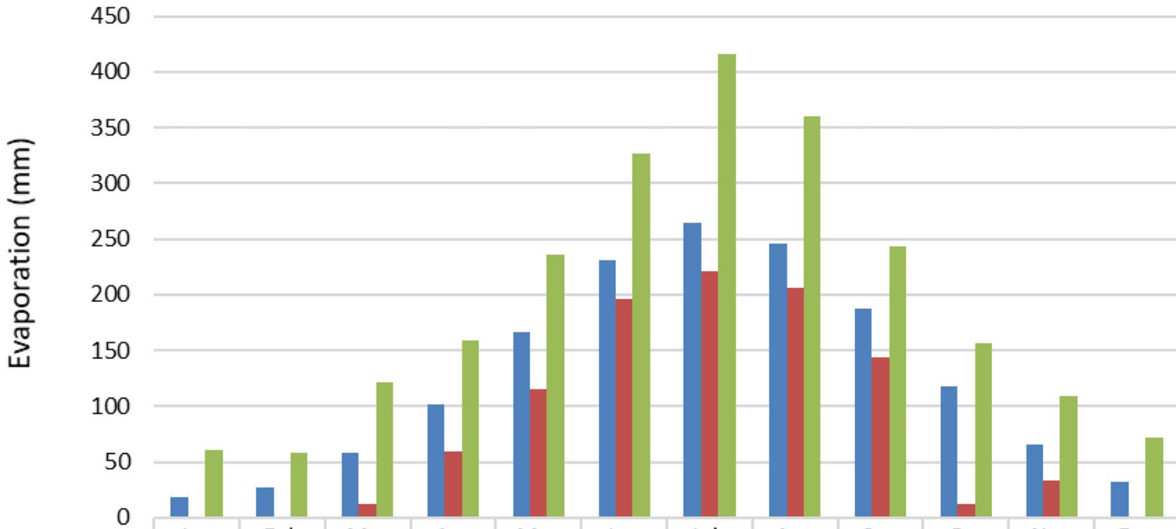

	Jan	Feb	Mar	Apr	May	Jun	July	Aug	Sep	Oct	Nov	Dec
average	18.3	26.8	57.8	101.9	166.3	231	263.8	246	187.5	117.8	65.1	32.5
minimum	0	0	11.6	59.5	114.7	196.3	221.4	206.5	144	11.6	33	0
maximum	60.1	58.4	121.5	159	235.6	327	415.4	359.6	243	156.4	108.5	72

Fig. 7 Average, minimum and maximum evaporation values for Odemis Station

Egri Creek

Egri Creek flows in northerly direction and joins the Kucuk Menderes River at the north. In the KMRB, there are eight stream gauging stations (see Fig. 8), where Kizilkaya-Egri Creek Station (06–42) operates adjacent to Egri Creek. Monthly average flow rate data (1989–2019 period) measured at the hydrological gauging station 06–42 were obtained from the State Water Works (DSI). The average monthly flow rates from 1986 to 2019 are, respectively, 0.069, 0.198, 0.836, 1.279, 1.670, and 1.483 m^3/s for October, November, December, January, February, and March. The minimum flow rate of $Q = 0.069\ m^3/s$ amounts to 1,073,080 m^3 available minimum water volume for a 6-month period. Hence, the Egri Creek discharge series reveal that 1 (one) million m^3 volume of water could be utilised for the groundwater recharge for a period of 6 months (rainy period), with a design discharge of 0.069 m^3/s. The details of the study area and the data collection and analysis can be obtained from Sahin (2022).

Field and laboratory test

Characterisation of the alluvium aquifer in the study area was carried out by establishing field and laboratory studies. SK-1 to SK-16 (total of 16) wells (Fig. 9) were drilled by the mud-rotary method to define the alluvium aquifer lithology and to determine the hydraulic properties of the vadose zone of the study area. The soil samples were taken by the soil penetration test (SPT) method. The depth of the research wells ranged from 26 to 148 m, with a total length of about 1020 m, and the diameter of each well was 122 cm. The distance between the pumping wells and the observations varied from 25 to 100 m.

Pumping tests were carried out for about 24 h at some wells (namely, wells 1, 3, 6, 8, 13, and 15; see Fig. 9), and the drawdowns were observed in the other wells, presented in Fig. 10. The average hydraulic conductivity and storage coefficients were calculated by the aquifer test pro program (AQTESOLV) (http://www.aqtesolv.com/groundwater_flow_modeling.htm), which uses the Neuman method with

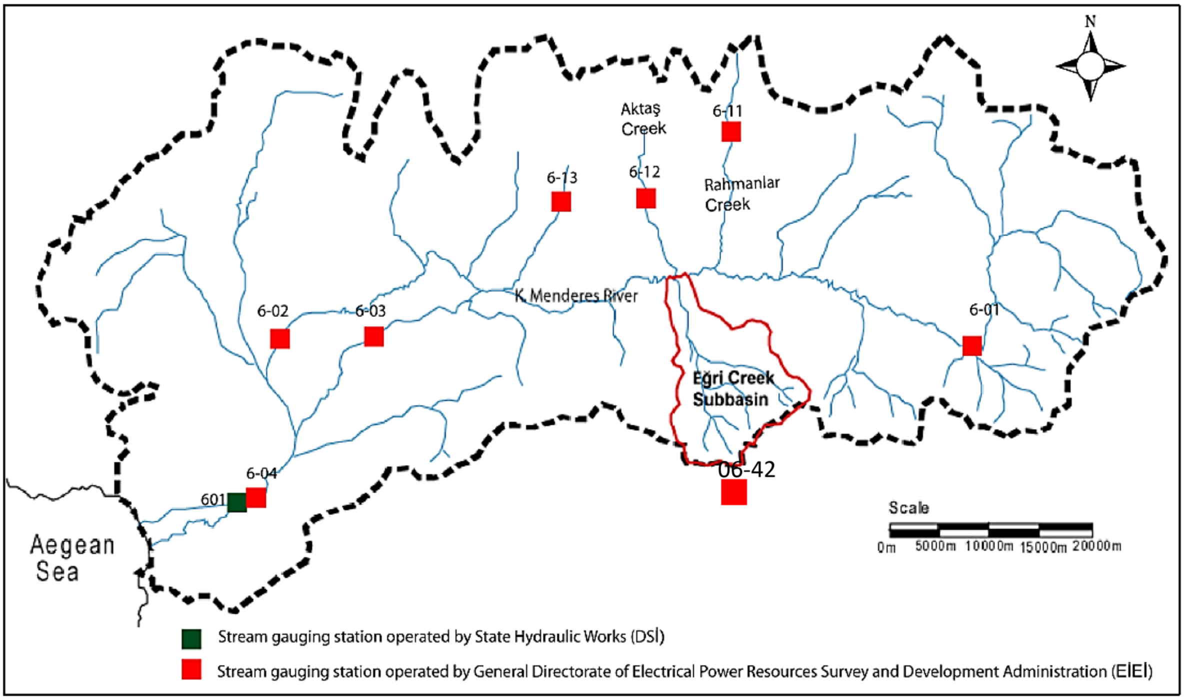

Fig. 8 Flow measurement stations in the Kucuk Menderes River Basin

the Jacob correction formula (Moench, 1993; Neuman, 1974; http://www.aqtesolv.com/theis-unconfined.htm#Jacob_Correction).

The saturated hydraulic conductivity values varied from 1.3 to 7.2 m/day. Table 1 presents hydraulic conductivity (K) and storativity (S), and the transmissivity (T) values for each observation well in the study area. To determine the distribution of hydraulic conductivity (K) values in the study area (see Fig. 10) the ordinary Kriging method was used. The details of the laboratory and field works can be obtained from Sahin (2022).

In the laboratory, the hydraulic properties of the alluvium aquifer were determined. The water content values ranged from 1.5 to 14.9%, and the specific gravity (Gs) of soil samples was also determined, ranging from 2.73 to 2.69. The range for porosity varied from 0.34 to 0.42. The sieve analysis was carried out to determine the variation of coarse- and fine-grained soils of the alluvial material in the study area. Sediment sizes ranged from 0.075 to 4.75 mm. The permeability tests in laboratory were carried out with constant head permeability tests on coarse-grained soils, while falling head permeability tests were applied on fine-grained units such as sand and clay. The range of results was between 2.55×10^{-5} and 5.30×10^{-4} m/s. The van Genuchten equations (Nielsen et al., 1986; van Genuchten, 1980) were employed to obtain the unsaturated hydraulic conductivity values that ranged from 0.049 to 0.0108 m/day.

Numerical model

This study employed HYDRUS-3D model to simulate the interaction of the SSR and the UDR with the flow in saturated–unsaturated zone. The model numerically (Galerkin type finite elements) solves Richards's equation in three dimensions. The model boundaries were determined from both the geological and hydrogeological characteristics of the study area. Since HYDRUS-3D uses a 3D representation of the subsurface, in this study, a length of about 1 km from the recharge pool centre in north–south and east directions is considered. Egri Creek is defined as the natural boundary on the west side. The distance of Egri Creek to the centre of the recharge pool is about 90 m, and the thickness of the domain ranges from 26 to 148 m. The specific yield of the model domain is

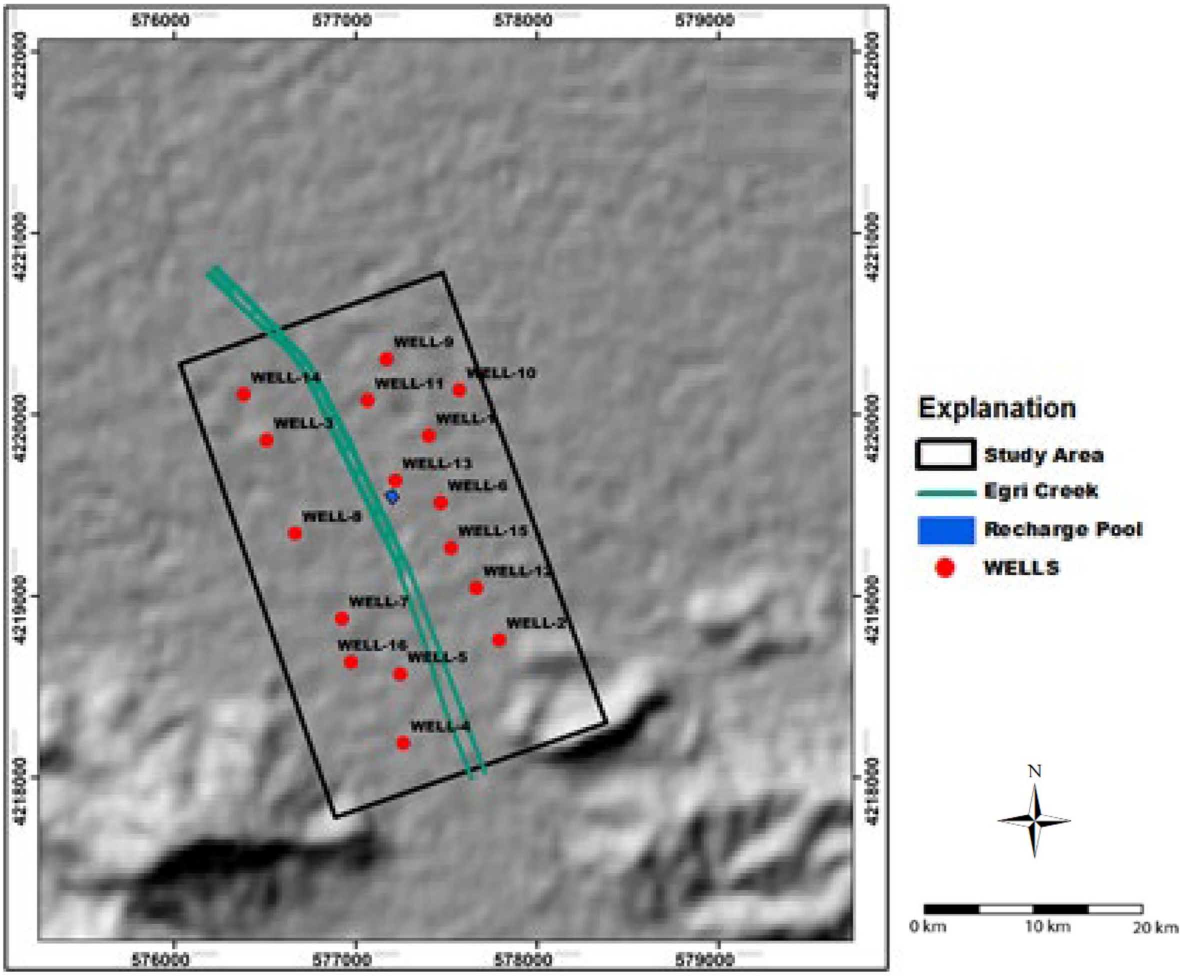

Fig. 9 Well locations in the study area

$S_y = 0.15$. The details of the numerical modelling can be obtained from Sahin (2022).

Figure 11 schematically represents the boundary conditions considered for the study area for the numerical model. Based on the data obtained from the geological and the hydrogeological investigations, the model domain is defined by the schist and gneiss at the bottom while the alluvial fan materials are considered in the other directions. Basically, the schist and gneiss are represented by no flow boundary (denoted by 1 in Fig. 11). The artificial recharge pool represents a constant head (3 m) boundary condition (denoted by 2 in Fig. 11) (3 m) during the simulation period (180 days). The infiltration of recharge water is modelled in 3D by the constant head boundary condition, and thus the upper part of the domain is represented by a ground surface (atmospheric boundary) (Fig. 11), which is exposed to meteorological events, and thus the atmospheric boundary condition (denoted by 3, Fig. 11) was chosen to represent Odemiş Meteorological Station data. Northern, southern, eastern, and western parts of the study area are expressed with free-flow-flux-type boundary condition (denoted by 4 in Fig. 11), which represents flow of water out of the system. Egri Creek was represented as the constant flux (specified head (denoted by 5 in Fig. 11)) boundary condition.

The initial conditions of the model were expressed in terms of water content and pressure head, respectively, as $\theta(z,t) = \theta_i(z,0)$ and $h(z,t) = h_i(z,0)$. The water content values of the vadose zone determined in

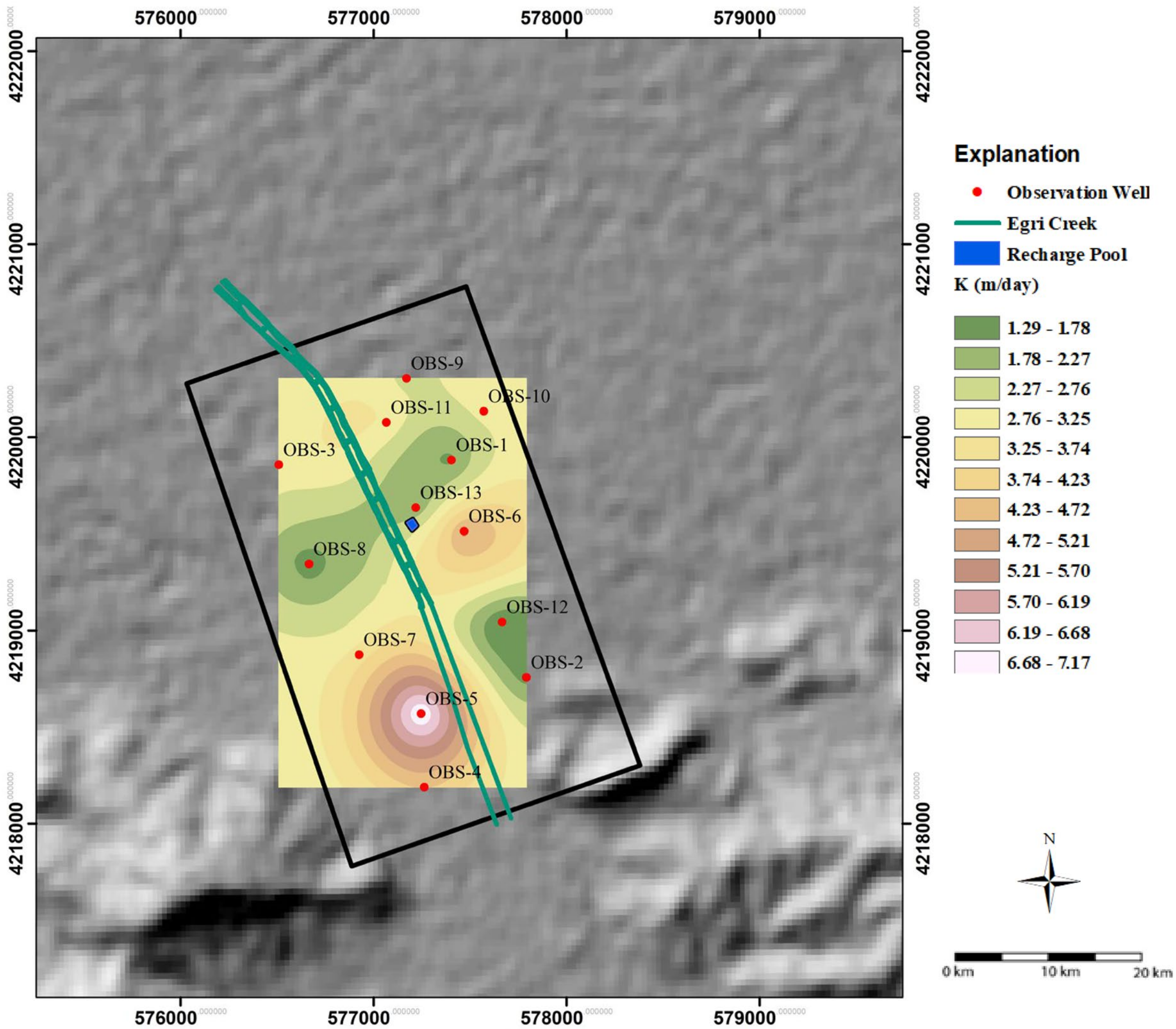

Fig. 10 Location of the observation wells and the distribution of *K*-values

the laboratory were used in the study as an initial condition. According to field and laboratory results, the lowest located nodal point of unsaturated zone was (z) 35 m, and thus, HYDRUS set the pressure at the bottom of the domain as equal to 35 m. The pressure head at the top of the domain would thus be equal to − 35 m since the domain has a depth of 70 m.

In order to obtain the most suitable mesh size and shape, the trial-and-error method was used, where the effect of each mesh type on the solution was investigated. As a result, the mixed type gave the best results and hence was selected. The element size in the model was assigned as 5 m with a width of 0.5 m, which resulted in 3606 nodes and 14,815 3D elements. Figure 12 shows the west-to-east cross-section distribution of finite element mesh along the domain. Since the response of the water table to the recharge is critical, a smaller mesh size was used.

Estimation of underground storage volume

Underground storage volume can be calculated by using the geological characteristics and elevation-area-volume curve of a studied area. First, several boreholes can be drilled in the intended area to obtain information on lithology. By the SPT method, several soil samples can be taken to a laboratory to

Table 1 Measured *K* and *S* values

Observation well	*S*	*K* (m/day)	*T* (m^2/day)
1	0.11	3.2	275.2
2	0.086	4.84	412
3	0.1	2.6	221
4	0.0219	1.6	129
5	0.34	3	335
6	0.23	1.5	171
7	0.22	1.7	192.1
8	0.32	3.5	392
9	0.13	4.3	527.5
10	0.095	7.2	878.5
11	0.24	4.6	561.2
12	0.21	1.3	171
13	0.079	3	335
Average	**0.15**	**3.26**	**372.1**

obtain soil characteristics and void ratio. Longitudinal profile of an underground dam reservoir can be obtained based on the bore log data. Elevation-area-volume curve can be constructed for the studied area. Then, the amount of water that can be stored can be easily predicted by simply multiplying the volume by the existing void ratio.

Numerical model validation

The groundwater table profiles from October 2018 to April 2019, obtained from the field measurements of water levels in three observation wells (SK_K27, SK_K6, and AK-5, see Fig. 13), were used to test the capability of the numerical model. The simulation covered a period of 180 days. This period corresponds to a wet season during which no pumping took place for irrigation purposes. In the model, the initial conditions were specified by water table elevations in October 2018; the model computed the necessary initial pore water pressures or head conditions from the assigned water table. The groundwater recharge for the corresponding period was assigned as a constant head boundary condition (a constant recharge pool depth of 3 m) and the daily Odemis Station meteorological data from October 2018 to April 2019 as the atmospheric boundary condition.

SK_K27 is located near the recharge pool, while SK_K6 is located on the east side, about 63 m away from the pool, and AK-5 is in the north side, about a distance of 165 m from the pool (see Fig. 13). Figures 14, 15, and 16 present the model simulations of heads observed in the three wells. As seen, the model is overall capable of predicting the levels satisfactorily, with the average $R^2=0.95$. The capturing of the heads at SK_K27 is satisfactory (see Fig. 14) with $R^2=0.99$, RMSE = 0.39 m, and MAE = 0.34 m, while there are slight underpredictions for simulated levels at SK_K6 ($R^2=0.96$, RMSE = 0.89 m, and MAE = 0.77 m) and AK_5 ($R^2=0.90$, RMSE = 1.56 m, and MAE = 1.46 m) (see Figs. 15 and 16). As the distance becomes longer, the underprediction of the heads becomes dominant. Also, soil formation sometimes includes a small amount of clay content, but not in the form of thick bands or lenses. One of the reasons for the low correlation may be that the presence of clay lenses causes a delay in groundwater motion. Also, as presented in Fig. 17, the groundwater contours tend to move towards nearly northwest, where AK_5 and SK_K6's locations are not corresponding to that direction. The numerical simulation, especially for AK_5 (Fig. 16), may be improved by providing a very fine resolution of the most sensitive parameter Ks (the saturated hydraulic conductivity) to the numerical model. However, such an approach may bring more burden on time, budgetary, and CPU constraints. Nevertheless, the simulations are, overall, considered to be satisfactory, implying that the numerical model is capable of simulating groundwater level changes as a result of surface spreading recharge in a field scale using rough field data.

Model application: artificial recharge scenarios

The validated numerical model was then applied to investigate recharge scenarios such as the surface spreading by using a recharge basin with different dimensions and by designing an underground dam. Note that there is a 1 million m^3 limitation in the surface water resource of Egri Creek for the 6-month period from October to April, as it was discussed above (see the "Egri Creek" section). The simulations were conducted for a period of 180 days between October 2018 and April 2019, where the same initial and boundary conditions were employed.

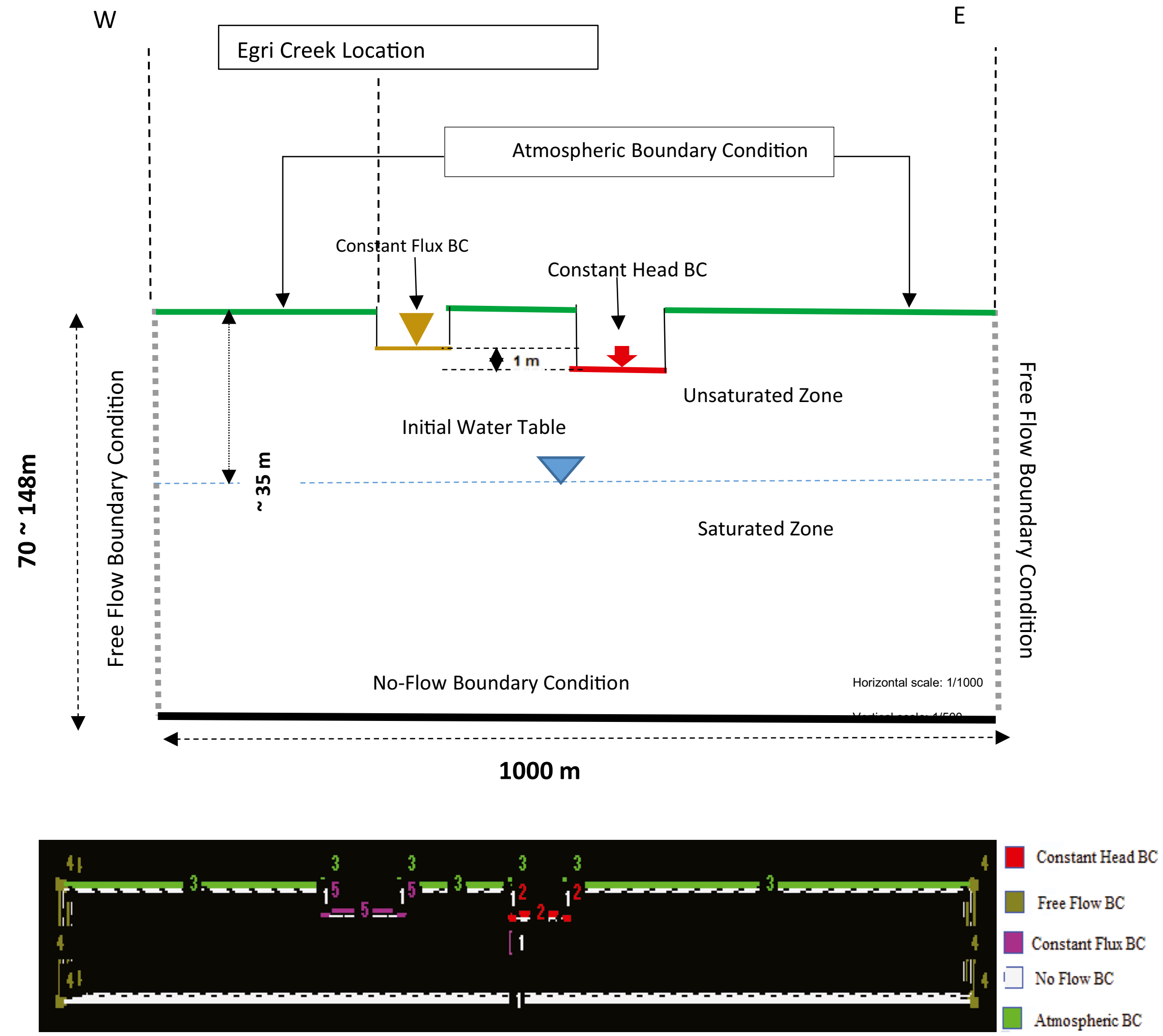

Fig. 11 Cross section W-E location and 2D view of boundary conditions

Recharge basin scenarios

Recharge basin design involves the construction of a basin to collect the diverted water from the Egri Creek regulator. The dimensions of the basin were determined by the site tests to check the available space for the construction, with a limiting factor that the depth of recharge basin should not exceed 6 m to provide the stability. Furthermore, minimum depth is considered to be 3 m. The average initial groundwater level is approximately 35 m. Table 2 summarizes considered seven scenarios and shows the effect of different sizes of recharge pools on the groundwater level. As seen, the average groundwater level increases due to increasing pool size from 12.5 to 34.1 m. Scenario 4, which involves a single 30 m by 30 m-sized basin with a 6 m depth, is considered to be the ideal one, under the constraints of soil stability and the availability of one million m^3 of water.

Underground dam scenario

Underground dams are also considered an artificial recharge method that prevents groundwater flow and store water beneath the ground (Nilsson, 1988). They

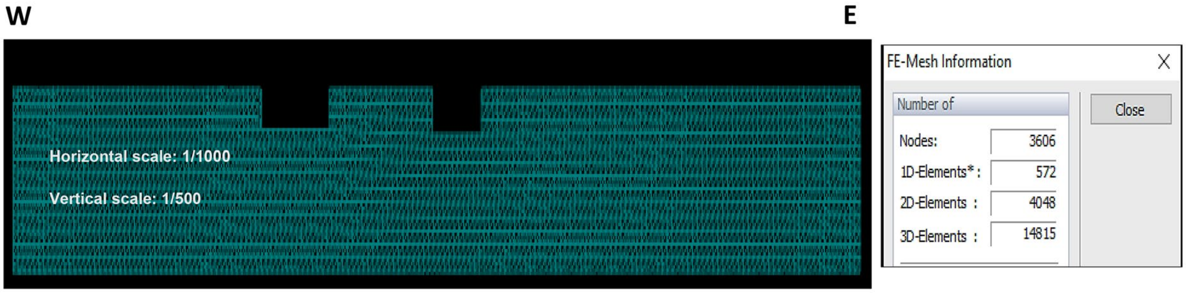

Fig. 12 Finite element mesh along the W-E domain

can enhance the storage of recharged water in the system by reducing or eliminating outflow from the system. They can be used in places where surface storage becomes impractical owing to high evaporation rates, reservoir siltation, and pollution risks. Although this technology is not new, its efficiency and simplicity have revived interest. Underground dams are constructed in well-defined and narrow valleys.

Hydrogeological and topographic investigations have revealed that the Egri Creek subbasin is suitable for an underground dam application where there exists alluvium in a 175-m-wide strip. For the conceptualised dam, an impermeable curtain can be constructed as 109 pieces of interlocking plaster strip, socketed into the bedrock on the slopes. The height between the talweg and the crest level is considered to be 23 m, with a total crest length of 196 m. The distance between the study area edge and the dam axis (upstream) is considered to be 680 m.

The underground dam storage capacity was calculated using the geological characteristics and the related elevation-area-volume curve of the studied area. Using the bore logs in the field, information on the lithology of the medium and the longitudinal profile of the underground dam reservoir was obtained. Then, for each 1 m height of the dam body (up to 23 m since the total height is 23 m), the related elevation-area-volume curve was constructed. Based on the soil characteristics obtained from the related soil samples of the studied area,

Fig. 13 Location of three observation wells

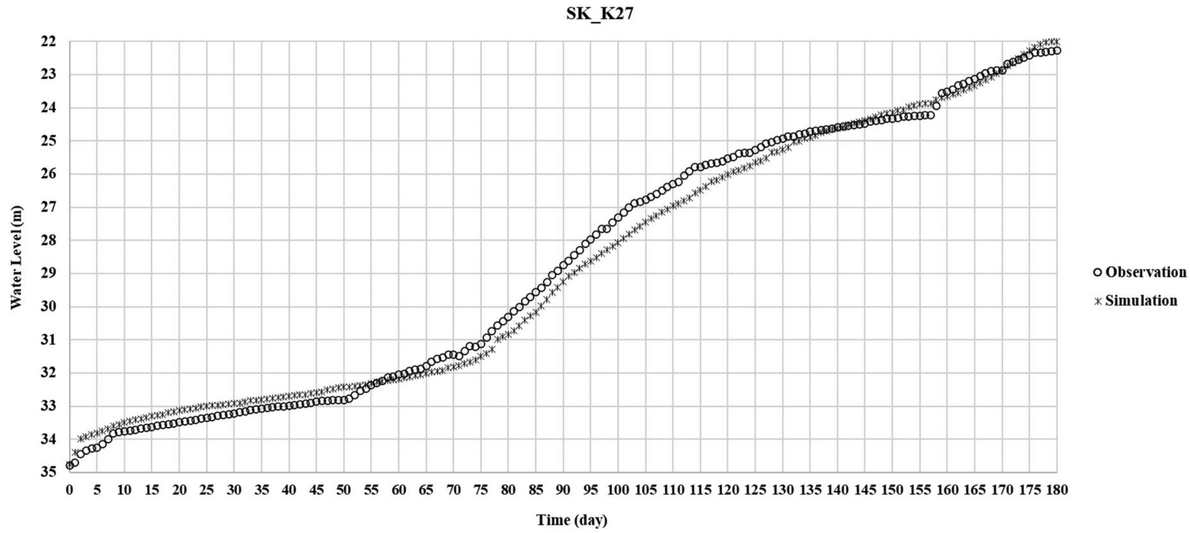

Fig. 14 Simulated and observed GWLs for SK_K27 well

the amount of water was predicted by multiplying the volume by the void ratio. Table 3 shows the accumulated (stored) water volume (m^3) of the underground dam depending on the level. Figure 18 shows the storage volume (m^3) corresponding to the reservoir elevation (m). As seen, the volumes and levels increase in the upstream direction. This field analysis reveals that the dam theoretically can store almost 720,500 m^3 of water.

Figure 19 presents the location of the conceptualised underground dam for numerical analysis. The model domain was selected with the help of Google Earth maps, and it was illustrated in the ArcGIS environment (see Fig. 20). The suitable region was chosen accordingly in the southern part of the system in the direction of underground flow where alluvial thickness is low and where water is not allowed to escape by design requirements.

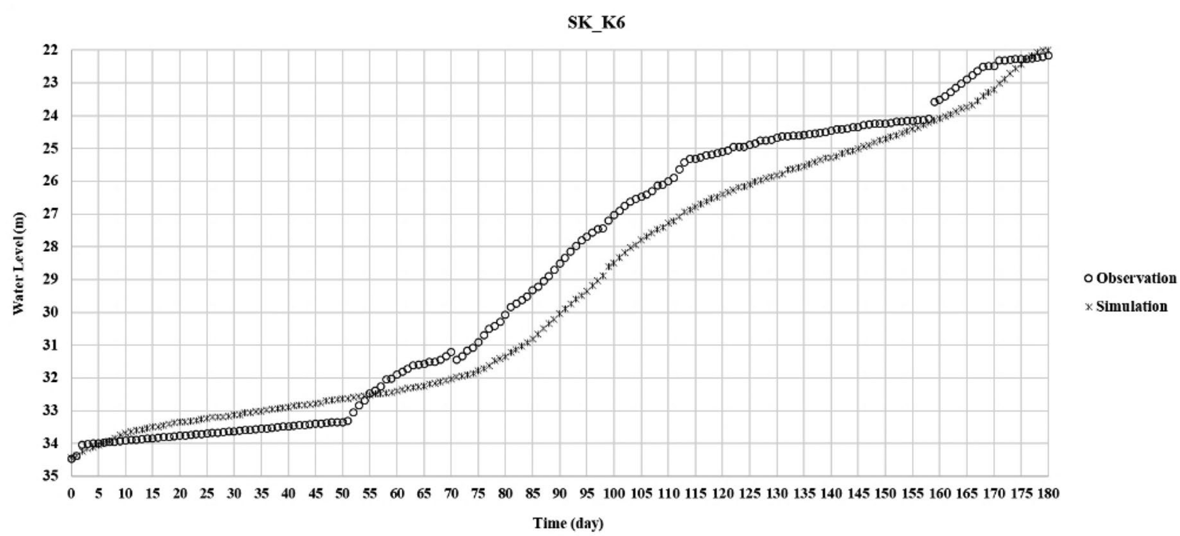

Fig. 15 Simulated and observed GWLs at SK_K6 well

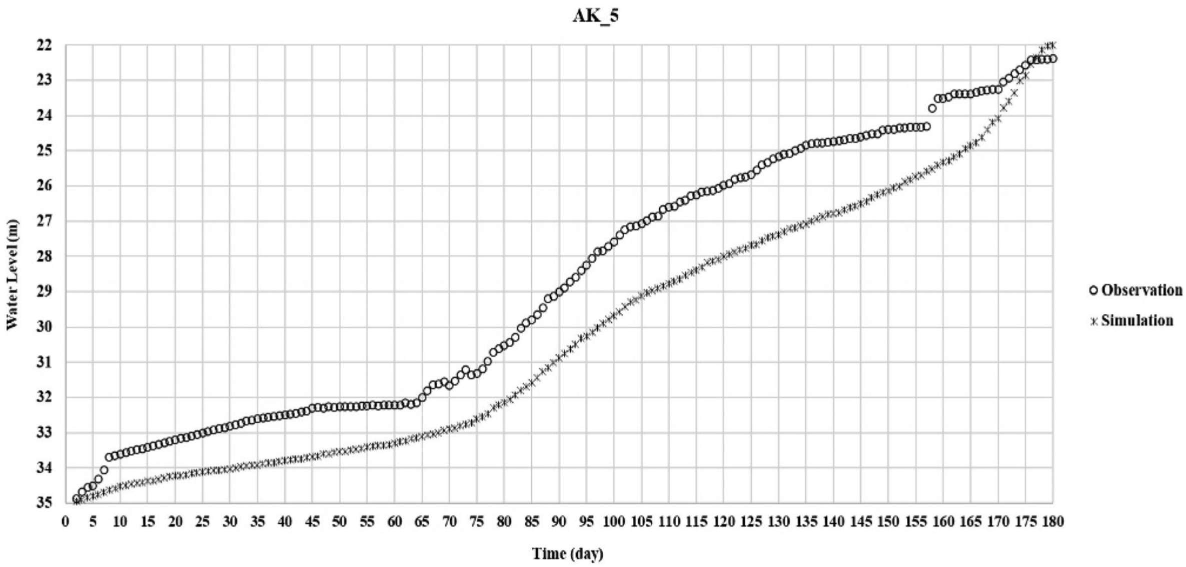

Fig. 16 Simulated and observed GWLs at AK_5

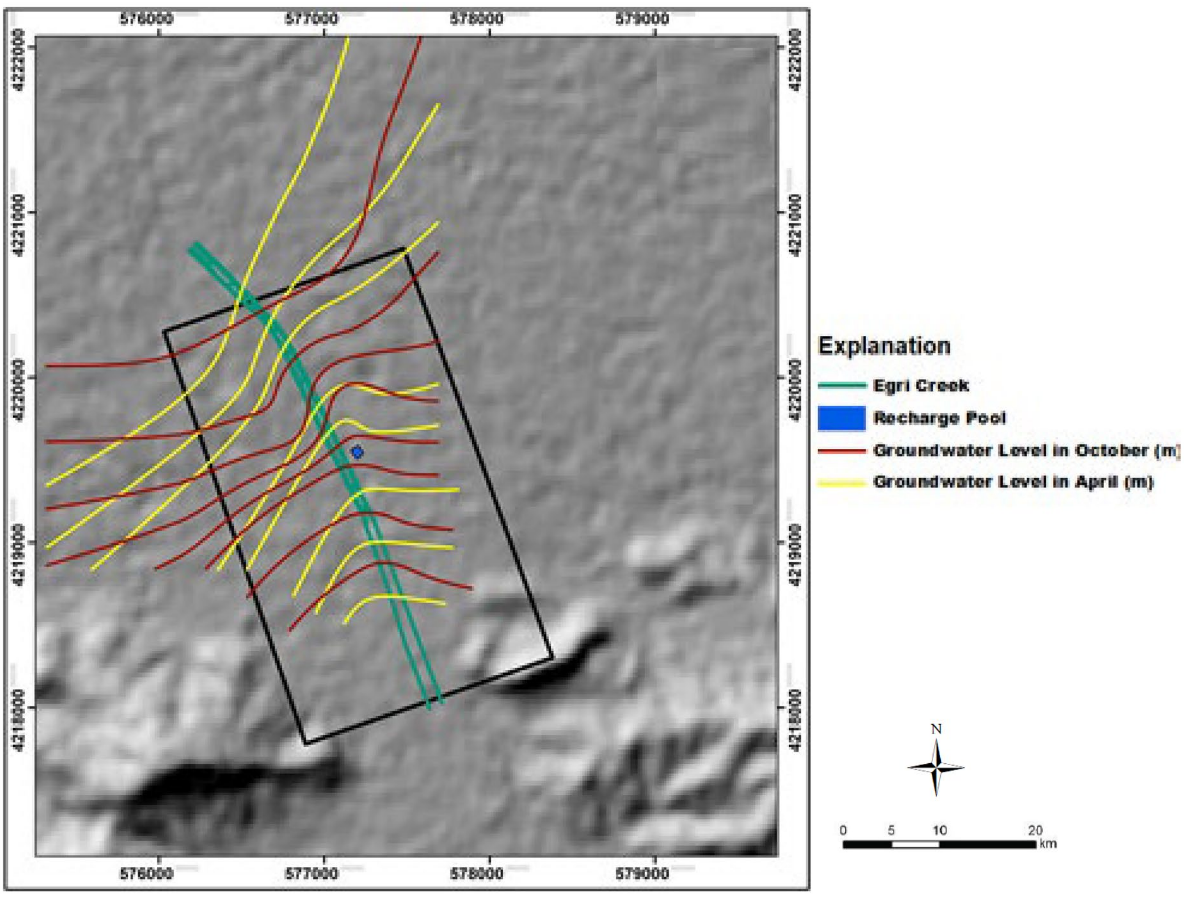

Fig. 17 Groundwater level distribution map created using the site tests

Table 2 Depth of recharge water and corresponding hydraulic level in recharge basin for different recharge basins and dimensions

Scenario	Number of basin	Dimensions (m)	Depth (m)	Daily average recharge (m^3)	Cumulative recharge (m^3)	Average increase of groundwater level (m)
1	1	6×6	3	1207	212,270	12.5
			4	1423.1	256,150	13.1
			5	1532.7	275,880	13.7
			6	1912.9	344,320	14.2
2	1	10×10	3	1957.2	352,300	13.8
			4	2403.1	432,550	14.6
			5	2712.5	488,250	16.1
			6	2816.6	506,990	16.8
3	1	20×20	3	3729	671,220	17.8
			4	3983.2	716,980	18.4
			5	4531.7	815,710	21.7
			6	5517.4	963,140	22.8
4	1	30×30	3	5350.4	964,770	25.1
			4	5363.2	965,380	26.5
			5	5374.9	967,480	27.6
			6	5446.7	980,440	29.3
5	1	50×50	3	6561.7	1,181,100	30.6
			4	6918.3	1,245,300	31.5
			5	7661	1,379,000	33.9
			6	7777.8	1,400,000	34.1
6	2	6×6	3	2257.8	406,400	14.4
			4	2767.4	498,130	16.2
			5	3275.7	589,620	17.3
			6	3859.2	694,650	18.1
7	2	10×10	3	5902.2	1,062,400	19.9
			4	6136.4	1,104,600	22.0
			5	6673.9	1,201,300	22.8
			6	7075.6	1,273,600	23.1

The numerical model boundaries were determined from both geological and hydrogeological characteristics of the study area. Based on the data obtained from geological and previous hydrogeological investigations and cross-sections, the model domain was defined by the schist and gneiss in the western, eastern, and at the bottom, while alluvial fan materials overlain on the bedrock (schist).

The ground surface is exposed to meteorological events, and hence the atmospheric boundary condition is chosen to represent Odemiş Meteorological Station data. Eastern and Western parts of the study area are expressed with no flow boundary condition since these parts correspond to mountains. Flow rate in Egri Creek is defined as the constant flux boundary condition. The model basement is defined as the no-flow boundary condition due to the presence of a schist layer. In the numerical model, the underground dam is simulated at the downstream edge (i.e. along the northern boundary), where flow of water out of the system is prohibited.

Simulation period begins on October 2018 and ends on April 2019. For the numerical modelling, the element size in the model was assigned as 3 m with a width of 1 m, which resulted in 150 nodes and 388 elements (see Fig. 21).

Table 3 Underground dam volume (m^3)–elevation (m) values

Volume ($\times 10^3$ m^3)	Elevation (m)
0	138
9.0	139
15.4	140
88.5	141
109.1	142
151.9	143
193.1	144
204.6	145
236.3	146
268.3	147
300.4	148
312.8	149
355.4	150
388.3	151
421.4	152
424.6	153
427.9	154
430.9	155
453.0	156
498.8	157
542.7	158
546.7	159
651.1	160
720.5	161

The rise in groundwater storage equals the amount of infiltration due to precipitation and the percolation from the creek base. The SS basin is located on the downstream side of the dam reservoir (see Fig. 22), and therefore there is no contribution from the SS basin. During the numerical analysis of the underground dam storage, the SS was considered to be inactive. The observation points (denoted as 1 to 11) were assigned to the model area randomly (see Fig. 22) to assess the simulation. The distance of the observation points from the underground dam axis are, respectively, 650, 600, 580, 550, 450, 350, 600, 400, 250, 100, and 30 m. As seen, the groundwater levels in the upstream direction of the underground dam show a significant increase (Fig. 23). The underground dam raises the groundwater level to a maximum value of 12.6 m at the point # 11, which is located 30 m away from the dam body. The groundwater rise, on the average, is about 9.5 m, considering all the observation points.

Although the related elevation-area-volume curve (see Fig. 18 and Table 3) indicates that about 720,500 m^3 volume of water may be stored in the specified field, the numerical model analysis results, on the other hand, reveal that the optimum storage volume would be 580,000 m^3.

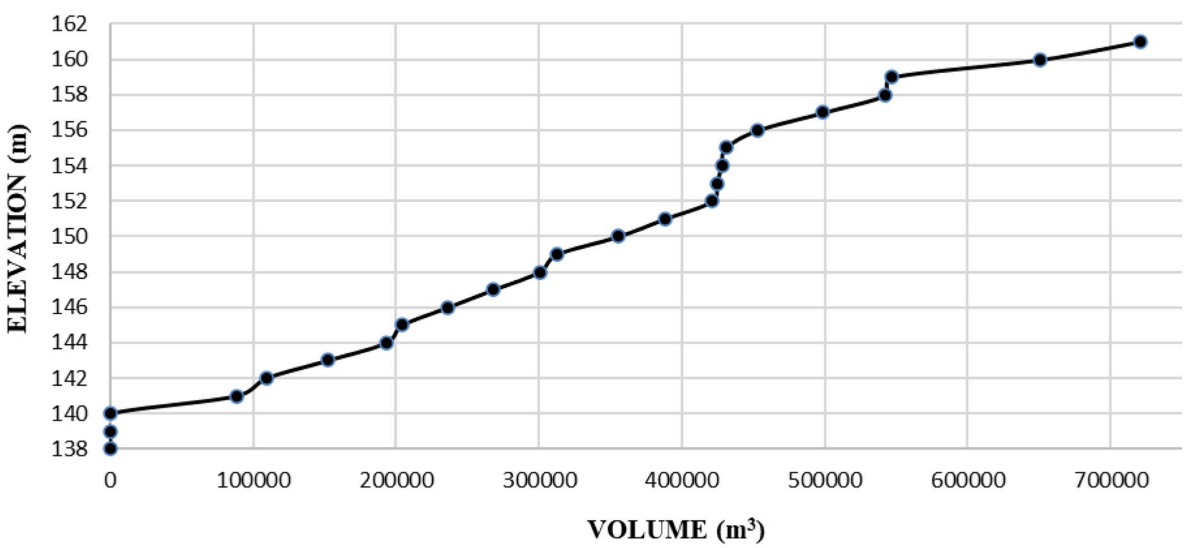

Fig. 18 Underground dam reservoir elevation (m)–volume (m^3)

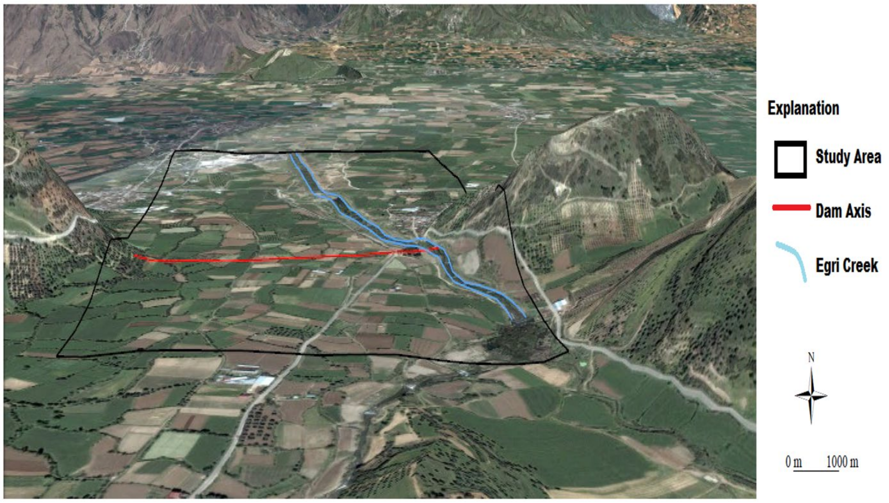

Fig. 19 Picture of the area where an underground dam is conceptualised (the map from Google Earth)

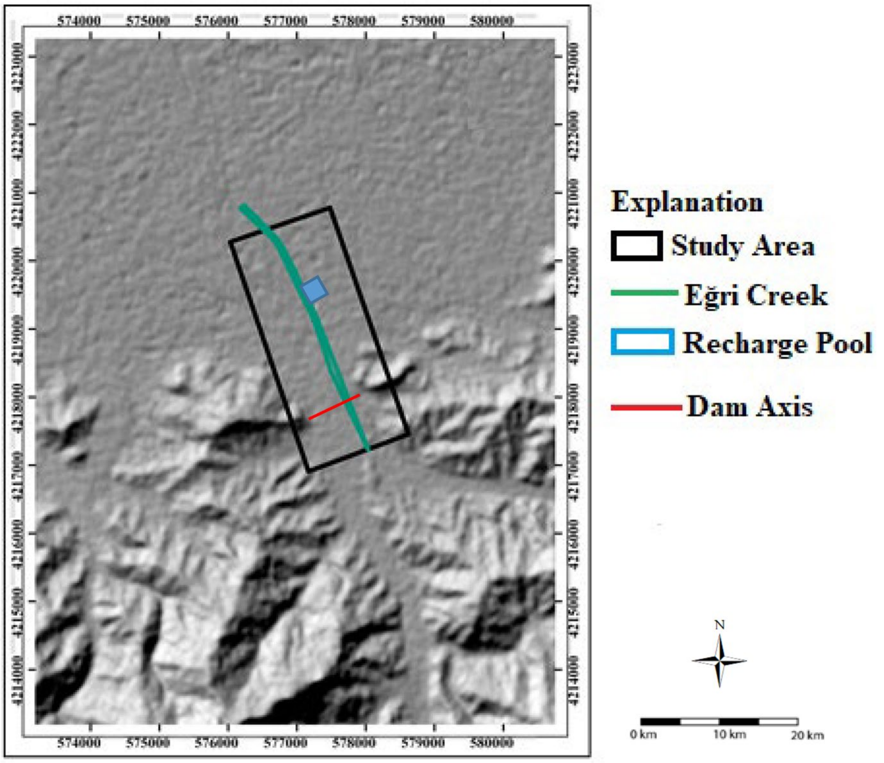

Fig. 20 Location of conceptualised underground dam

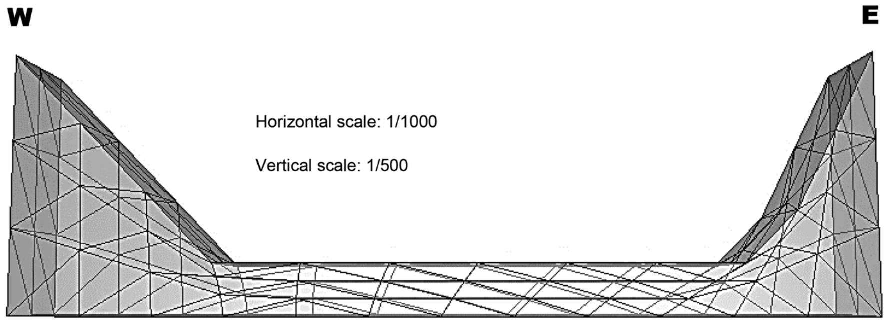

Fig. 21 Finite elements mesh along the dam axis

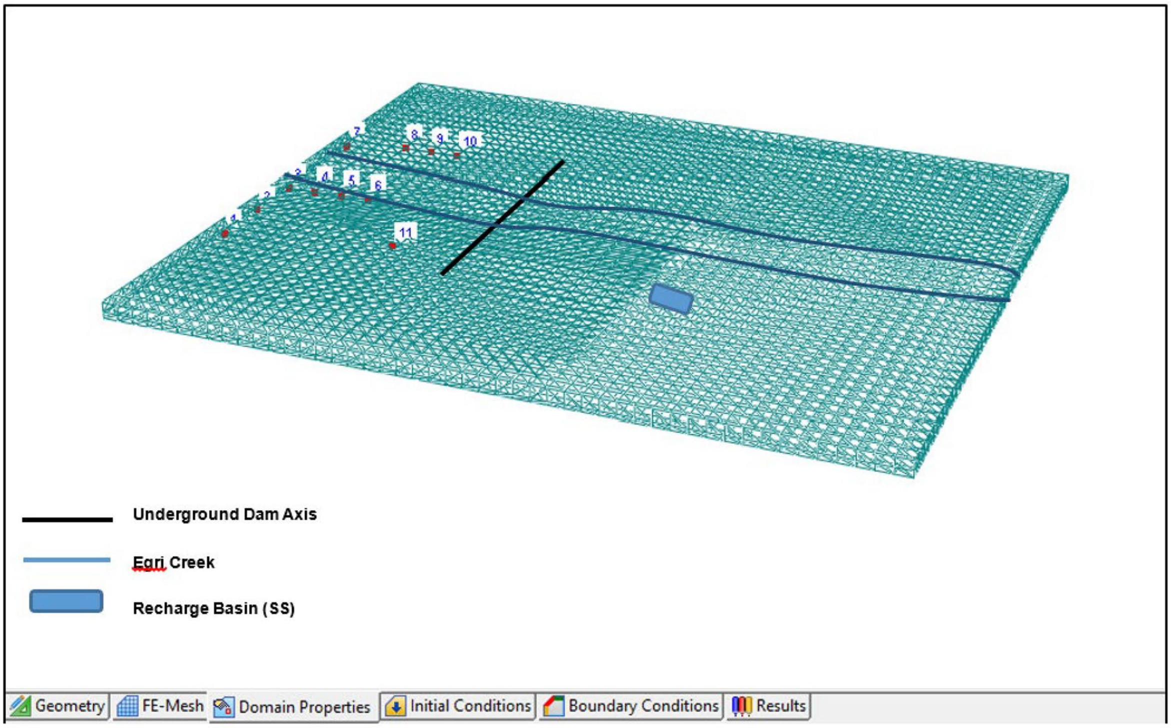

Fig. 22 The observation points in the model domain

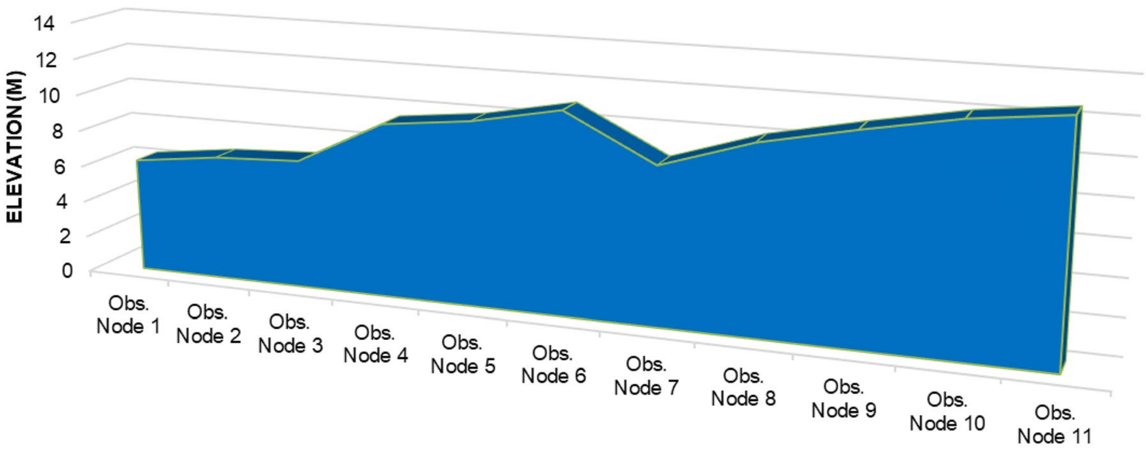

	Obs. Node 1	Obs. Node 2	Obs. Node 3	Obs. Node 4	Obs. Node 5	Obs. Node 6	Obs. Node 7	Obs. Node 8	Obs. Node 9	Obs. Node 10	Obs. Node 11
Water Elevation (m)	6.22	6.795	7.021	9.43	9.968	10.923	8.486	10.059	11.087	12.012	12.57

Fig. 23 Water table elevation corresponds to observation points

Summary and conclusions

This study investigates the artificial recharge of groundwater in the Egri Creek subbasin of the Kucuk Menderes Basin in Izmir, Turkey. Discharge values for Egri Creek are obtained from the hydrological gauging station. The lithology and parameters of hydrogeological data are obtained from the boreholes scattered in the study area. Water potential used for the artificial recharge basin is limited due to the upstream hydraulic projects. The design flow rate is found to be 69 l/s and the amount of water to be diverted amounts to 1 million m^3/year. Three-dimensional numerical model, HYDRUS, is employed for investigating the recharge from the surface spreading basin and the underground dam.

The results indicate that the proposed recharge pool design procedure is effective at augmenting groundwater levels. The simulation results show that groundwater table elevations rise in different levels (12.5 to 34.1 m) depending upon the dimension of the recharge pool. However, due to the limitation on the water supply, and the stability issue of the recharge pool design, the most suitable one is found to be scenario 4 recharge basin, which has a depth of 6 m and dimensions of 30 m (length) by 30 m (width). Such a recharge pool can raise the groundwater level by an average of 29.3 m.

Three-dimensional numerical analysis of recharge due to an underground dam reveals that there could be about a 580,000 m^3 increase in groundwater storage. The groundwater level increases more rapidly at points close to the dam axis. The underground dam raises the groundwater level by an average of 9.3 m, which may not be sufficient to warrant the construction of an underground dam.

It is also worth noting that the operation and maintenance cost of the underground dam is more expensive than the artificial groundwater basin recharge basin. Furthermore, the construction time of the underground dam is longer than that of the artificial recharge basin. Also, in terms of the application technique, the underground dam requires a more detailed and delicate design. The artificial groundwater basin recharge project is cheaper and easily applicable.

This research can lead to new studies on the applicability of artificial recharge of groundwater in different parts of the world, including Turkey, using the surplus flow of rivers during the rainy season. The research can be extended to study various effects of artificial recharge of groundwater, e.g. land subsidence prevention.

Author contribution All authors contributed to the study's conception and design. Material preparation, data collection, and analysis were performed by Yavuz Sahin. The first draft of the manuscript was written by Gokmen Tayfur, and all authors commented on previous versions of the manuscript. All authors read and approved the final manuscript.

Availability of data and materials Authors have no restrictions on sharing data and/or any material.

Declarations

Ethical approval All authors have read, understood, and complied, as applicable, with the statement on "ethical responsibilities of authors" as found in the instructions for authors and are aware that, with minor exceptions, no changes can be made to authorship once the paper is submitted.

Consent to participate Not applicable.

Consent for publication The authors have approved the manuscript submission.

Competing interests The authors declare no competing interests.

References

Al-Muttair, F. F., & Al-Turbak, A. S. (1991). Modeling of infiltration from an artificial recharge basin with decreasing ponded depth. *Journal of King Saud University-Engineering Sciences, 3*, 89–100.

Apaydın, A. (2009). Malibogazi groundwater dam: An alternative model for semi-arid regions of Turkey to store and save groundwater. *Environmental Earth Sciences, 59*, 339–345.

Apaydin, A. (2014). Underground dams-from site selection to operation. DSI Publications, ISBN: 978-605-64763-0-3, Ankara, Turkey. (In Turkish).

Boochs, P. W., & Billib, M. (1994). Management of a small ground water reservoir by recharge water from a surface reservoir. In: Johnson, A.I. and Pyne, D.G., (eds.). *Proceedings of the Second International Symposium on Artificial Recharge of Groundwater*, 661–668.

Bouwer, H. (2002). Artificial recharge of groundwater: Hydrogeology and engineering. *Hydrogeology Journal, 10*, 121–142.

DSI. (2016). Kucuk Menderes River Basin master plan report, technical report prepared by the State Water Works (DSI), Ankara, Turkey. (in Turkish).

DSI Records. (2019). The State Water Works (DSI) groundwater level records. DSI Branch in Izmir, Turkey. (in Turkish).

Foster, S., & Tuinhof, A. (2004). Brazil, Kenya: Subsurface dams to augment groundwater storage in basement terrain for human subsistence. *Sustainable Groundwater Management Lessons from Practice, Case Profile Collection, 5*, 1–8.

Gelebo, A. H., Kasiviswanathan, K. S., & Khare, D. (2022). Assessment of the spatial–temporal distribution of groundwater recharge in data-scarce large-scale African river basin. *Environmental Monitoring and Assessment, 194*, 157. https://doi.org/10.1007/s10661-022-09778-z

Izbicki, J. A., Flint, A. L., & Stamos, C. L. (2007). Artificial recharge through a thick, heterogeneous unsaturated zone. *Ground Water, 46*(3), 475–488.

Jarraya-Horriche, F., Benabdallah, S., & Ayadi, M. (2020). Groundwater monitoring for assessing artificial recharge in the Mediterranean coastal aquifer of Korba (Northeastern Tunisia). *Environmental Monitoring and Assessment, 192*, 442. https://doi.org/10.1007/s10661-020-08408-w

Kimrey, J. O. (1989). Artificial recharge of groundwater and its role in water management. *Desalination, 72*, 135–147.

Light, M. E. (1994). Design, construction, and operation of a surface recharge facility for the purpose of reusing secondary effluent in an arid climate, Tucson, Arizona, USA. In: Johnson, A.I. and Pyne, D.G., (eds.). *Proceedings of the Second International Symposium on Artificial Recharge of Groundwater*, 342- 351.

Masoud, M. H. Z., Basahi, J. M., & Zaidi, F. K. (2019). Assessment of artificial groundwater recharge potential through estimation of permeability values from infiltration and aquifer tests in unconsolidated alluvial formations in coastal areas. *Environmental Monitoring and Assessment, 191*(31). https://doi.org/10.1007/s10661-018-7173-6

Moench, A. F. (1993). Computation of type curves for flow to partially penetrating wells in water-table aquifers. *Ground Water, 31*(6), 966–971.

Neuman, S. P. (1974). Effect of partial penetration on flow in unconfined aquifers considering delayed gravity response. *Water Resources Research, 10*(2), 303–312.

Nielsen, D. R., Th. Van Genuchten, M., & Biggar, J. W. (1986). Water flow and solute transport processes in the unsaturated zone. *Water Resources Research, 22*(9), 89–108.

Nilsson, A. (1988). *Groundwater dams for small-scale water supply* (p. 69). Intermediate Technology Publications.

Phillips, S. P. (2003). Aquifers, artificial recharge of. *Encyclopedia of Water Science, 1*(1), 33–36.

Reddy, K. R. (2008). Enhanced aquifer recharge. In: Darnault, C.J.G. (ed.). *Overexploitation and Contamination of Shared Groundwater Resources*, 275–287.

Richter, R. C., & Chun, R. Y. D. (1959). Geologic and hydrologic factors affecting infiltration rates at artificial recharge sites in California. In: Schiff, L. (ed.). Bienn. Conf. on ground-water recharge, 2d, Berkeley, Calif., Proc: Collins, Colo., Western Soil and Water Management Research Br., 48–52.

Sahin, Y. (2022). Three dimensional numerical modelling of recharge: Case study: Eğri creek sub-basin, İzmir. PhD Dissertation, Izmir Institute of Technology, Izmir, Turkey.

Sayit, A. P., & Yazicigil, H. (2012). Assessment of artificial aquifer recharge potential in the Kucuk Menderes River Basin, Turkey. *Hydrogeology Journal, 20*(4), 755–766. https://doi.org/10.1007/s10040-012-0850-6

Schiff, L., & Dyer, K. L. (1964). Some physical and chemical considerations in artificial ground-water recharge. *International Association of Scientific Hydrology, 64*, 347–358.

Siebert, S., Burke, J., Faures, J. M., Frenken, K., Hoogeveen, J., Döll, P., & Portmann, F. T. (2010). Groundwater use for irrigation – A global inventory. *Hydrology and Earth System Sciences, 14*(1863–1880), 2010. https://doi.org/10.5194/hess-14-1863-2010

Van Genuchten, MTh. (1980). A closed form equation for predicting the hydraulic conductivity of unsaturated soils. *Soil Science Society of America Journal, 44*, 892–898.

Yagbasan, O. (2016). Impacts of climate change on groundwater recharge in Kucuk Menderes River Basin in Western Turkey. *Geodinamica Acta, 28*(3), 209–222. https://doi.org/10.1080/09853111.2015.1121802

Yazicigil, H., Doyuran, V., Karahanoğlu, N., Yanmaz, M., Çamur, Z., Toprak, V., Rojay, B., Yılmaz, K. K., Şakıyan, J., Süzen, L., Yeşilnacar, E., Gündoğdu, A., Pusatlı, T., & Tuzcu, B. (2000). Investigation and management of groundwater resources in Küçük Menderes River Basin under the scope of revised hydrogeological studies, Project no: 98–03-09-01-01. Middle East Technical University.